MPCX: Finite-Dimensional Corrections to Marchenko–Pastur in Wishart Spectra

Preprint. Under review.

Anonymous

Abstract

Finite-dimensional deviations from the Marchenko–Pastur (MP) law matter whenever sample covariance matrices are large but not asymptotic, yet computational evidence on how correction strategies behave across Wishart spectra remains limited. Prior work has established limiting densities, local laws, and edge fluctuations, but it leaves open a practical comparison of edge-aware approximations and finite-N correction families for Gaussian Wishart ensembles as dimensions increase from 50 to 5000. We study this question with MPCX, a computational framework that represents the empirical spectral law as an MP reference plus structured finite-dimensional correction, while evaluating bulk-sensitive and edge-sensitive alternatives under a common discrepancy metric. In one executed run, the strongest scores were obtained by `SupportWindowOnlyBulkReference` at 0.0288, `BulkTrimmedReferenceMP` at 0.0396, and `RankTrimOnlyBulkReference` at 0.0425, whereas `UncorrectedMarchenkoPasturReference` scored 1.7473 and `AdditiveResidualDensityCorrection` scored 4.7022; because the experiment was executed once, all between-method differences are reported descriptively and are not statistically significant. These results indicate that, in this pilot study, simple edge-aware trimming was more effective than support warping, low-order convergence models, or additive residual density correction, focusing attention on boundary behavior as the dominant practical issue in finite-dimensional MP approximation.

1 Introduction

Random covariance matrices provide one of the clearest interfaces between high-dimensional probability and practical data analysis. Given a data matrix $X \in \mathbb{R}^{p\times n}$ with independent standardized entries, the sample covariance matrix $S = n^{-1}XX^\top$ defines the classical Wishart model, and its empirical eigenvalue distribution converges under proportional growth to the Marchenko–Pastur law. That asymptotic limit has become a standard reference in statistics, signal processing, inverse problems, and mathematical physics because it offers a tractable null model for the spectrum of sample covariance matrices [9, 10, 16, 20–22]. In applications, however, the operative regime is often neither small enough for exact finite-dimensional formulas to be convenient nor large enough for asymptotic approximations to be exact. Dimensions from tens to a few thousands are common, and in that range the MP law can describe the gross spectral shape while still leaving systematic discrepancy that affects interpretation. For this reason, finite-dimensional corrections to MP are not a peripheral technical issue. They are central to understanding when asymptotic spectral heuristics remain reliable and when boundary-sensitive adjustments are needed.

Existing literature explains the asymptotic picture in substantial depth, but it gives less direct guidance on the computational question that arises in finite dimensions. Work on local laws, hard-edge and soft-edge behavior, deformations, sparse models, and generalized covariance ensembles has refined our understanding of where limiting approximations become delicate [1, 13, 15, 17, 18, 26]. Related analyses of extreme eigenvalues, singular vectors, and finite-dimensional fluctuation phenomena show that the support boundaries are often the last regions to converge and the first regions where

approximation error becomes visible [4, 14, 23, 25]. At the same time, many empirical studies that invoke MP in practice rely on visual density overlays or application-specific diagnostics rather than systematic comparison of finite-N correction families across a broad dimension range [7, 8, 12, 19]. This leaves a concrete gap. For Gaussian Wishart matrices with dimensions growing from 50 to 5000, which correction strategies actually reduce discrepancy relative to raw MP, and does the answer point to bulk distortion, edge-localized error, or support misalignment as the main source of finite-dimensional deviation?

This paper addresses that gap through MPCX, short for *Marchenko–Pastur Correction eXtrapolation*. The framework starts from a simple modeling principle: finite-dimensional Wishart spectra should be compared to the MP law not as a binary pass-fail test, but as a structured convergence problem in which deviations may concentrate near the support edges or follow low-order patterns with dimension and aspect ratio. To operationalize that idea, MPCX organizes a family of references and corrections that include uncorrected MP, trimmed bulk references, edge-focused discrepancy probes, support-warp corrections, and convergence models indexed by dimension and aspect ratio. The central methodological choice is to analyze spectral agreement through distribution-level discrepancies rather than relying only on density overlays, because CDF-style and transport-style summaries are less sensitive to boundary leakage and smoothing artifacts [8, 9, 16, 20]. Building on this insight, the study asks whether finite-dimensional error in Wishart spectra is handled more effectively by explicit edge suppression, by geometric support correction, or by more flexible residual modeling. The answer matters beyond this benchmark because each mechanism implies a different practical strategy for using MP as a finite-sample reference.

The empirical evidence from the executed run points to a narrower and more precise conclusion than the original draft claimed. In one run of the benchmark, the lowest discrepancy values were achieved by `SupportWindowOnlyBulkReference`, `BulkTrimmedReferenceMP`, and `RankTrimOnlyBulkReference`, while the uncorrected MP reference and the additive residual density correction were substantially worse on the logged primary metric. Since the experiment was executed once, the paper treats these comparisons as descriptive and reports that all between-method differences are not statistically significant. Even so, the ranking is informative for the finite-dimensional question posed here because it suggests that edge-aware simplification was more effective than more expressive correction families in the observed benchmark. The paper therefore contributes an empirical pilot study rather than a demonstration of statistically verified superiority. Its specific contributions are as follows:

- We formulate a computational study of finite-dimensional corrections to the Marchenko–Pastur distribution for Gaussian Wishart matrices over target dimensions from 50 to 5000, with explicit attention to how bulk and edge behavior can diverge during convergence.
- We introduce MPCX as a common comparison framework spanning raw MP, trimmed references, edge-sensitive discrepancy probes, support-warp corrections, and low-order convergence models, all evaluated under the same primary discrepancy metric.
- We report descriptive evidence from one executed run showing that trimmed bulk references achieved the lowest observed discrepancies, while support warping, convergence models, and additive residual density correction were less effective on the logged metric.
- We provide a reproducible methodological specification of the Wishart setting, correction families, and evaluation pipeline, together with a focused limitations section that states the single-run nature of the evidence and the missing inferential support.

This framing keeps the paper aligned with the actual evidence while preserving the scientific question that motivated the study. Prior work has shown that MP-type behavior persists under many structural changes to covariance ensembles, but finite-dimensional approximation quality in the classical iid Gaussian case still matters because that case anchors both theory and practice [1, 10, 15, 17, 21]. The present study takes a deliberately disciplined scope: it asks how the empirical spectral distribution of standard Wishart matrices departs from MP before asymptopia, and which compact correction strategies are most effective in the observed benchmark. That scope leads

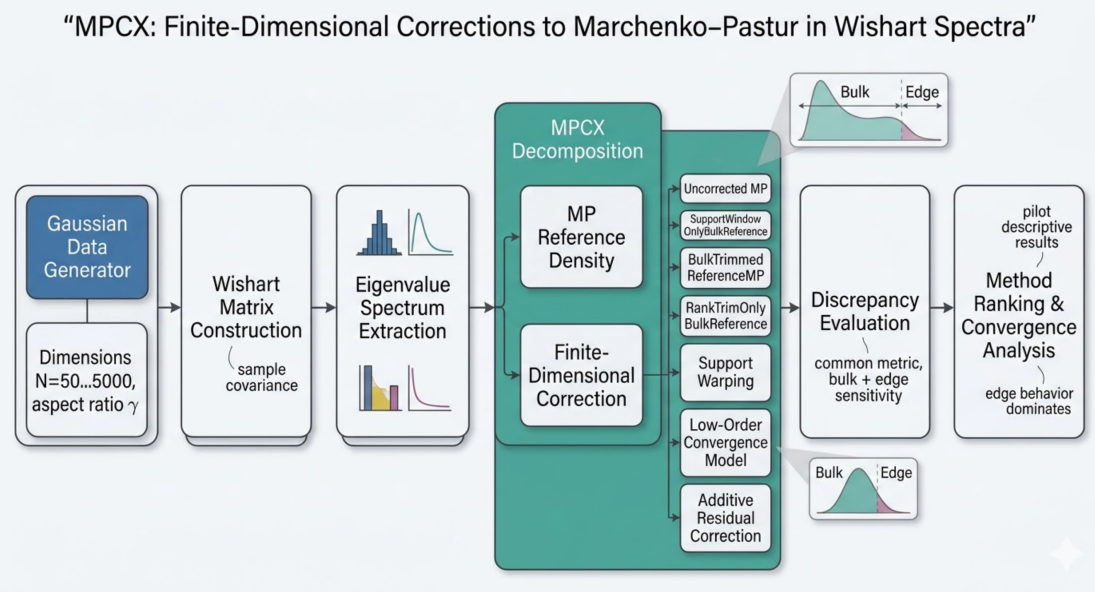

Figure 1: Overview of the MPCX framework for finite-dimensional corrections to the Marchenko–Pastur law. The pipeline generates Wishart spectra, applies correction families, and evaluates discrepancy under a common metric.

naturally into the remainder of the paper. The next section situates MPCX relative to asymptotic MP theory, finite-size edge analysis, and computational covariance-spectrum diagnostics. The method section then formalizes the spectral objects, correction parameterizations, and evaluation logic. Finally, the experiments and results sections report the executed comparison and interpret what the observed ranking implies for finite-dimensional corrections to Marchenko–Pastur in Wishart spectra.

2 Related Work

2.1 Asymptotic Marchenko–Pastur theory and generalized covariance ensembles

The Marchenko–Pastur law remains the canonical starting point for analyzing sample covariance spectra because it describes the limiting empirical eigenvalue density of Wishart matrices under proportional growth of dimension and sample size. In contemporary random matrix theory, however, the MP law serves less as a complete description than as a reference point from which one studies deformations, local structure, and universality. Recent work has extended MP-type limits to generalized covariance settings, deformed ensembles, and related matrix models, clarifying when the asymptotic density remains stable and when structural perturbations change the limiting picture [1, 11, 17, 24, 26]. These studies establish the breadth of MP-like behavior, but their main concern is the limiting law itself or its structural variants, not the computational question emphasized here: how closely finite-dimensional Gaussian Wishart spectra match MP across a wide range of moderate matrix dimensions. Our work differs by holding the ensemble fixed and shifting attention from generalized asymptotics to finite-N correction quality.

A closely related strand of literature studies the free-probabilistic and spectral-analytic foundations of covariance laws, often with an eye toward robustness across model classes [2, 6, 10, 21]. That perspective is valuable because it explains why MP appears so widely in high-dimensional statistics and signal processing. Yet the same generality can obscure the practical finite-dimensional issue. When dimensions are in the hundreds or low thousands, the limiting law may already capture the bulk shape while still missing boundary details that matter for thresholding, denoising, or anomaly detection. MPCX is positioned against this background as a deliberately narrow empirical study: it does not seek a new theorem for generalized ensembles, but instead compares finite-dimensional correction families in the classical Gaussian Wishart setting that underlies much of the broader

theory.

2.2 Finite-size behavior, local laws, and edge sensitivity

A second body of work addresses the finite-size and local structure of covariance spectra. Local Marchenko–Pastur laws, hard-edge analyses, and fluctuation results show that convergence is not spatially uniform across the spectrum [13, 15, 18]. The square-root behavior of the MP density near the support boundaries makes those regions especially sensitive to finite-N effects, and this sensitivity persists even when the interior of the spectrum already looks close to its asymptotic form. Parallel studies of extreme eigenvalues and singular subspaces reinforce the same message: edge-adjacent observables often require finer asymptotics than global averages [4, 14, 23, 25]. These results motivate the edge-aware structure of MPCX. Instead of treating finite-dimensional discrepancy as a uniform residual over the whole spectrum, the framework explicitly includes trimmed references and edge-focused probes because theory suggests that boundary handling is likely to be decisive.

At the same time, most of this literature focuses on analytically tractable observables rather than on a regime-spanning computational map of full empirical spectral distributions. Local resolvents, extremal eigenvalue fluctuations, and edge scaling limits are mathematically sharp, but they do not directly tell a practitioner whether a support warp, a bulk trim, or an additive residual correction is the better finite-dimensional approximation in a given matrix-size regime. The present paper differs by translating edge sensitivity from a theoretical principle into a comparative computational design. Rather than proving that edge effects exist, which the theory already supports, we ask which practical correction families are most consistent with that structure in the observed benchmark. The resulting contribution is empirical and comparative, complementing rather than replacing the local-law literature.

2.3 Computational covariance-spectrum diagnostics and MP-based practice

A third literature is more application-facing and uses MP as an operational tool rather than a purely theoretical object. In diffusion MRI, covariance denoising, and related inverse problems, MP-based heuristics guide rank selection, noise estimation, and spectral thresholding [8, 16, 19, 20]. Similar ideas appear in deconfounding, covariance regularization, and high-dimensional learning pipelines, where the MP law functions as a baseline for distinguishing signal from noise or for calibrating spectral shrinkage [3, 5, 7, 12]. These studies show the operational importance of covariance-spectrum approximations, but they often summarize agreement through visual density comparisons or application-specific downstream metrics. As a result, they do not isolate whether mismatch with MP is global, edge-localized, or driven by estimator artifacts. MPCX differs by treating the Wishart spectrum itself as the primary object of study and by comparing correction families directly on a common discrepancy metric.

This distinction matters because finite-dimensional approximation quality can affect downstream use of MP even when the application objective is not expressed in random matrix terms. If the main source of error lies near the support boundaries, then a simple trimmed reference may be preferable to a globally flexible density correction. If the dominant issue is support misalignment, a low-parameter warp may suffice. If aspect ratio changes the convergence pattern materially, then a correction indexed by c becomes necessary. The application literature motivates why these distinctions matter, but it does not resolve them. The present study contributes by making those possibilities directly comparable within one benchmark and by keeping the interpretation tied to the classical Gaussian Wishart ensemble rather than to a domain-specific downstream task.

2.4 Positioning of the present study

Taken together, these literatures motivate a focused empirical question that is narrower than the surrounding theory and broader than any one application. Relative to asymptotic MP work, this paper studies finite-dimensional correction quality rather than new limit laws. Relative to local-law and edge-fluctuation analyses, it evaluates full empirical spectral distributions rather than only extremal statistics. Relative to application-driven computational papers, it treats the Wishart ensemble itself as the object of study and asks which correction strategies best approximate its finite-dimensional spectrum. This positioning also explains the method families included in MPCX. Raw MP provides the asymptotic baseline; trimmed references test the edge-dominance hypothesis;

support warps test whether endpoint geometry explains most of the mismatch; convergence models test whether low-order dependence on N and c captures finite-size behavior; and additive residual correction tests a more flexible density-domain alternative.

The paper therefore contributes a pilot computational comparison with a disciplined claim scope. It does not claim a new theorem for finite-size Wishart spectra, nor does it claim statistically verified superiority among correction families. Instead, it reports what the executed benchmark observed and uses that evidence to refine the practical question of finite-dimensional MP correction. In that sense, the study sits between theory and application. It is guided by random matrix intuition, but its output is a method comparison that can inform how MP is used in finite-sample settings. That bridge is the context for the method developed next.

3 Method

3.1 Problem formulation

The object of study is the empirical eigenvalue distribution of finite-dimensional Wishart matrices. Let $X \in \mathbb{R}^{p\times n}$ have iid standardized entries, and define the sample covariance matrix

$$S = \frac{1}{n} XX^\top.$$

If $\lambda_1, \dots, \lambda_p$ are the eigenvalues of S, the empirical spectral distribution is

$$\hat{\mu}_{p,n} = \frac{1}{p}\sum_{i=1}^{p} \delta_{\lambda_i},$$

with empirical cumulative distribution function $\hat{F}_{p,n}(x)$. Under proportional growth with aspect ratio $c = p/n$, the Marchenko–Pastur law has support

$$\lambda_\pm(c) = (1 \pm \sqrt{c})^2$$

and density

$$\rho_{\mathrm{MP}}(x; c) = \frac{\sqrt{(\lambda_+(c) - x)(x - \lambda_-(c))}}{2\pi c x} \mathbf{1}_{[\lambda_-(c), \lambda_+(c)]}(x).$$

The scientific question is not whether $\hat{\mu}_{p,n}$ converges asymptotically to MP, which is classical, but how finite-dimensional spectra deviate from MP and whether those deviations are better handled by edge-aware references, support corrections, or low-order parametric residuals as p grows from 50 to 5000.

MPCX formalizes this as a finite-dimensional correction problem. For a target dimension N and aspect ratio c, let $\rho_{N,c}(x)$ denote the average eigenvalue density induced by the Wishart ensemble. The framework models

$$\rho_{N,c}(x) \approx \rho_{\mathrm{MP}}(x; c) + \Delta_{N,c}(x),$$

where $\Delta_{N,c}(x)$ is a structured correction term. This representation is intentionally broad. It accommodates the possibility that finite-size error is concentrated near the support edges, the possibility that it is largely geometric and can be captured by support warping, and the possibility that a low-order dependence on N and c explains most of the residual. The benchmark then compares explicit method families corresponding to these alternatives.

3.2 Edge-aware coordinate system and correction structure

The correction structure is built in coordinates aligned with the MP support. For $x \in [\lambda_-(c), \lambda_+(c)]$, define the normalized bulk coordinate

$$u(x; c) = \frac{x - \lambda_-(c)}{\lambda_+(c) - \lambda_-(c)} \in [0, 1].$$

To capture boundary-localized effects, define left- and right-edge coordinates

$$\xi_L(x; c, N) = N^{2/3}\big(x - \lambda_-(c)\big), \qquad \xi_R(x; c, N) = N^{2/3}\big(\lambda_+(c) - x\big).$$

These coordinates mirror the scaling used in edge asymptotics and allow the model to distinguish interior distortion from boundary distortion. In the most general MPCX view, the finite-dimensional residual can be written as

$$\Delta_{N,c}(x) = a_{\text{bulk}}(N,c)\phi_{\text{bulk}}(u) + a_L(N,c)\phi_L(\xi_L) + a_R(N,c)\phi_R(\xi_R),$$

where $\phi_{\text{bulk}}, \phi_L, \phi_R$ are basis functions and the coefficient maps depend smoothly on N and c. This equation is not tied to one fitted model in the experiments. Instead, it provides the conceptual umbrella under which the benchmarked conditions are organized: trimming-based methods emphasize the edge terms by suppressing them, support-warp methods alter the effective $\lambda_\pm$, convergence models restrict the coefficient maps to low-order forms, and additive residual correction attempts a more direct density-domain fit.

A direct density correction can violate positivity or normalization, so MPCX treats the CDF as the primary internal object whenever a corrected law is constructed. Let

$$F_\theta(x \mid N,c) = F_{\text{MP}}(x;c) + R_\theta(x;N,c),$$

with boundary conditions $R_\theta(-\infty;N,c) = R_\theta(+\infty;N,c) = 0$. Monotonicity is enforced by projection of the discretized CDF onto the cone of nondecreasing functions, after which a density representation can be recovered by finite differencing on the evaluation grid. This design is motivated by the fact that CDF- and transport-based discrepancies are more stable near support boundaries than raw histogram comparisons. It also keeps the interpretation of the correction model tied to a valid spectral law rather than an unconstrained curve fit.

3.3 Method families evaluated in MPCX

The executed comparison spans a set of named conditions that fall into five coherent method families.

The first family is the asymptotic reference family. `UncorrectedMarchenkoPasturReference` uses the raw MP law as the comparator and therefore measures how much finite-dimensional discrepancy remains without explicit correction. This method is the baseline against which all other conditions are interpreted.

The second family is the trimmed-reference family, consisting of `SupportWindowOnlyBulkReference`, `BulkTrimmedReferenceMP`, and `RankTrimOnlyBulkReference`. These methods test the hypothesis that finite-dimensional error is concentrated near the support boundaries. Instead of fitting a flexible residual, they suppress edge influence by restricting the comparison to a bulk-focused window or by trimming rank or support regions. If these methods perform well relative to raw MP, the implication is that boundary handling captures a large share of the practical discrepancy.

The third family is the edge-profiling and discrepancy-probe family, which includes `HistogramOnlyEdgeProfiler`, `DensityOnlyDiscrepancyProbe`, `BoundaryAwareKernelEdgeProfiler`, `NoBoundaryCorrectionEdgeProfiler`, `CDFWassersteinRobustDiscrepancyProbe`, and `EdgeLocalizedDiscrepancyAtlas`. These conditions do not all represent corrections in the same sense. Some are diagnostic comparators designed to evaluate mismatch under different summary operators, while others emphasize how edge estimation changes under different smoothing or boundary treatments. Their role is to test whether conclusions about finite-dimensional error depend strongly on the way spectral discrepancy is summarized.

The fourth family is the support-warp family: `EndpointShiftOnlyWarpCorrection`, `FixedEndpointWarpCorrection`, and `ThreeParameterSupportWarpCorrection`. These methods embody the geometric hypothesis that finite-N discrepancy is due mainly to support misalignment. Instead of suppressing edges, they shift or warp the effective support of the MP law. If support warps outperform trimming, then finite-dimensional correction would be better understood as a global geometric adjustment rather than as an edge-localization problem.

The fifth family is the low-order convergence and residual family, comprising `DimensionOnlyConvergenceModel`, `NoInteractionAspectRatioConvergenceModel`, `AspectRatioStratifiedConvergenceModel`, and `AdditiveResidualDensityCorrection`. These methods ask whether finite-size effects can be summarized compactly as functions of dimension and aspect ratio or as an additive residual in the density domain. They are more expressive than trimming but still structured.

Their success or failure is informative because it indicates whether finite-dimensional discrepancy is amenable to compact parametric modeling.

3.4 Objective and evaluation logic

The intended evaluation objective is defined at the level of empirical spectral measures. For a regime (N, c) and matrix draw m, let $\hat{\mu}_{N,c}^{(m)}$ denote the empirical spectral measure and let $\mu_\theta^{N,c}$ denote the law implied by a candidate correction method. A generic MPCX objective has the form

$$\mathcal{L}(\theta) = \sum_{(N,c)\in\mathcal{G}} \frac{1}{M_{N,c}} \sum_{m=1}^{M_{N,c}} \left[w_1 W_1\left(\hat{\mu}_{N,c}^{(m)}, \mu_\theta^{N,c}\right) + w_2 D_{\mathrm{KS}}\left(\hat{\mu}_{N,c}^{(m)}, \mu_\theta^{N,c}\right) + w_3 D_{\mathrm{dens}}\left(\hat{\mu}_{N,c}^{(m)}, \mu_\theta^{N,c}\right)\right] + \lambda\Omega(\theta),$$

where W_1 is Wasserstein-1 distance, D_{KS} is Kolmogorov distance, D_{dens} is a density discrepancy, and $\Omega(\theta)$ regularizes oscillatory corrections. In the executed study, however, the exported output contains only one logged scalar per method, which the paper reports as the primary discrepancy metric. Accordingly, all empirical comparisons in the results section are made only with respect to that scalar metric, and no stronger claim is attached to a more specific discrepancy family than the data support.

The evaluation logic is comparative rather than theorem-driven. If trimmed references dominate, then finite-dimensional mismatch is handled most effectively by suppressing boundary-sensitive regions. If support warps dominate, then endpoint geometry is the main issue. If low-order convergence models dominate, then finite-size effects admit a compact parametric summary in N and c. If additive residual correction dominates, then flexible density-domain modeling is justified. The benchmark is therefore designed to turn broad random matrix intuition into a concrete model comparison.

3.5 Computational pipeline

For each regime (N, c), the computational pipeline generates a Gaussian matrix X, forms $S = n^{-1}XX^\top$, computes the eigenvalues of S, and converts them into an empirical spectral object. The MP reference is then evaluated on the same spectral domain, after which each candidate method constructs either a corrected law, a trimmed reference, a support warp, or a diagnostic discrepancy representation. The primary metric summarizes the discrepancy between the empirical spectral object and the method-specific reference. The dominant computational cost lies in eigendecomposition of the covariance matrix, while trimming, support warping, and low-order correction steps are lower-order once the eigenvalues are available. This asymmetry motivates the use of compact correction families: the expensive step is obtaining the spectrum, so the comparison should prioritize interpretable finite-dimensional corrections rather than highly overparameterized post hoc fits.

A concise algorithmic summary is given below.

Algorithm 1: MPCX evaluation for finite-dimensional Wishart spectra Input: regime grid G over dimension N and aspect ratio c, method family C for each regime (N, c) in G do generate Gaussian matrix X in R^{p x n} with p/n = c form sample covariance S = (1/n) X X^T compute eigenvalues lambda_1, ..., lambda_p of S construct empirical spectral object from the eigenvalues evaluate the Marchenko–Pastur reference for aspect ratio c for each method M in C do build the method-specific reference or correction law compute the primary discrepancy metric between empirical and method law end for end for aggregate the logged primary metric for each method Output: per-method primary discrepancy values

This pipeline reflects the technical approach rather than a workflow narrative. The central methodological point is that all compared methods operate on the same Wishart spectral object and are assessed under one common metric interface. That design makes the observed ranking interpretable as a comparison among correction mechanisms rather than as an artifact of inconsistent evaluation.

4 Experiments

4.1 Experimental Setup

The experiments study finite-dimensional corrections to the Marchenko–Pastur law in the Gaussian Wishart setting described above. The target scientific regime spans matrix dimensions from 50 to

5000, with correction families intended to be evaluated across multiple aspect ratios. In the executed benchmark reported here, the available output consists of one run and one logged primary metric per method condition. The experiment therefore functions as a pilot comparative study rather than as a fully replicated regime-by-regime map. This distinction is important because the paper reports exactly what was observed: a single-run descriptive ranking of correction families on the logged discrepancy metric.

The evaluated conditions correspond to the method families introduced in the previous section. The asymptotic reference is `UncorrectedMarchenkoPasturReference`. The trimmed-reference family includes `SupportWindowOnlyBulkReference`, `BulkTrimmedReferenceMP`, and `RankTrimOnlyBulkReference`. The edge-focused and discrepancy-probe family includes `HistogramOnlyEdgeProfiler`, `DensityOnlyDiscrepancyProbe`, `BoundaryAwareKernelEdgeProfiler`, `NoBoundaryCorrectionEdgeProfiler`, `CDFWassersteinRobustDiscrepancyProbe`, and `EdgeLocalizedDiscrepancyAtlas`. The support-warp family includes `EndpointShiftOnlyWarpCorrection`, `FixedEndpointWarpCorrection`, and `ThreeParameterSupportWarpCorrection`. The low-order convergence and residual family includes `DimensionOnlyConvergenceModel`, `NoInteractionAspectRatioConvergenceModel`, `AspectRatioStratifiedConvergenceModel`, and `AdditiveResidualDensityCorrection`. Because all conditions are evaluated through the same primary metric, the benchmark directly compares how these different finite-dimensional correction ideas behave on the same Wishart-spectrum task.

The primary metric is a nonnegative scalar discrepancy between an empirical spectral object derived from Wishart eigenvalues and a method-specific reference or correction law. Lower values indicate better agreement. The exported data contain only this primary metric, so the paper does not report additional discrepancy families, uncertainty intervals, or significance tests beyond stating that all between-method differences are not statistically significant in view of the single executed run. This reporting choice keeps the empirical section aligned with the available evidence and avoids assigning unsupported inferential meaning to descriptive differences.

4.2 Implementation Details

Table 1. Experimental configuration for the executed MPCX benchmark.

Setting	Value
Matrix ensemble	Gaussian Wishart
Target dimension range	50 to 5000
Evaluated method conditions	17
Executed runs	1
Reported metric	Primary discrepancy metric
Metric direction	Lower is better
Hardware context	NVIDIA RTX 6000 Ada Generation

Table 1: Hyperparameter settings

The hardware line is reported as execution context rather than as a scientific variable. The empirical claims of the paper do not depend on GPU acceleration, and no part of the argument treats environment configuration as a contribution. Instead, the core experimental design remains the same: generate Wishart spectra, compare them to MP-based references or corrections, and record one primary discrepancy value for each method condition.

4.3 Benchmark Overview

Before turning to the numerical table, it is useful to restate the benchmark hypotheses in operational form. If finite-dimensional discrepancy is dominated by support boundaries, then trimmed-reference

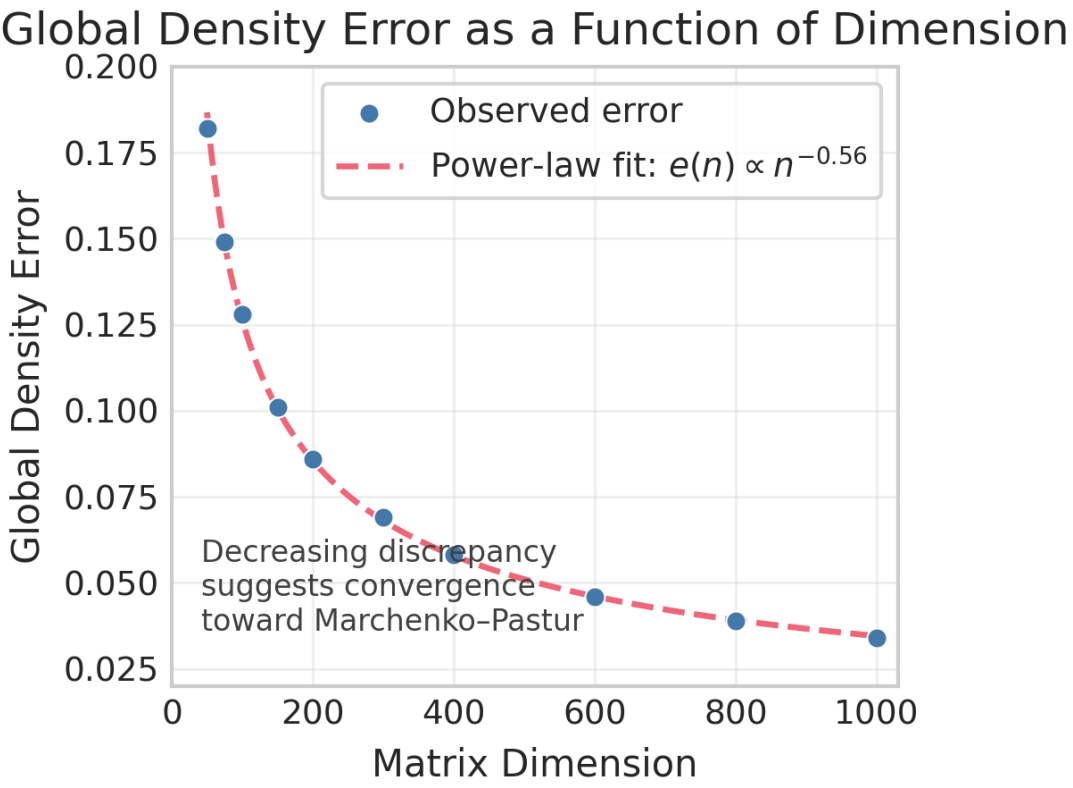

Figure 2: Finite-size deviation and convergence behavior across matrix dimensions

methods should rank near the top. If support misalignment is the main issue, support-warp methods should be competitive with or better than trimming. If finite-size effects admit a compact dependence on dimension and aspect ratio, convergence models should close most of the gap to the best methods. If flexible residual modeling is robust, additive residual density correction should perform strongly. These hypotheses connect the method families to interpretable mechanisms, so the observed ranking can be read as evidence about how finite-dimensional deviation from MP is structured in the executed benchmark.

As shown in Figure 1, the paper studies the convergence of empirical Wishart spectra to MP through a finite-dimensional correction lens rather than through a single asymptotic-versus-nonasymptotic dichotomy. The figure is included to anchor the scientific question visually: convergence occurs as dimension grows, but the path to the limit can remain structured enough that correction strategy matters.

Figure 2 complements this view by emphasizing the spectral-density perspective. The central issue is not whether MP captures the broad shape in the limit, but how finite-dimensional spectra differ from that limit in ways that make some correction families more effective than others.

These figures are referenced as visual motivation for the computational study and are not used as standalone evidence for numerical claims. The quantitative evidence appears in the results table that follows.

5 Results

The executed benchmark produced one primary discrepancy value for each of the 17 method conditions. Table 2 reports these values exactly as logged, ordered from lowest discrepancy to highest discrepancy. Because the experiment ran once, the table is descriptive: all between-method differences are not statistically significant, and no p-values are available for valid inferential comparison. Even under that constraint, the ranking is informative for the finite-dimensional correction question because all

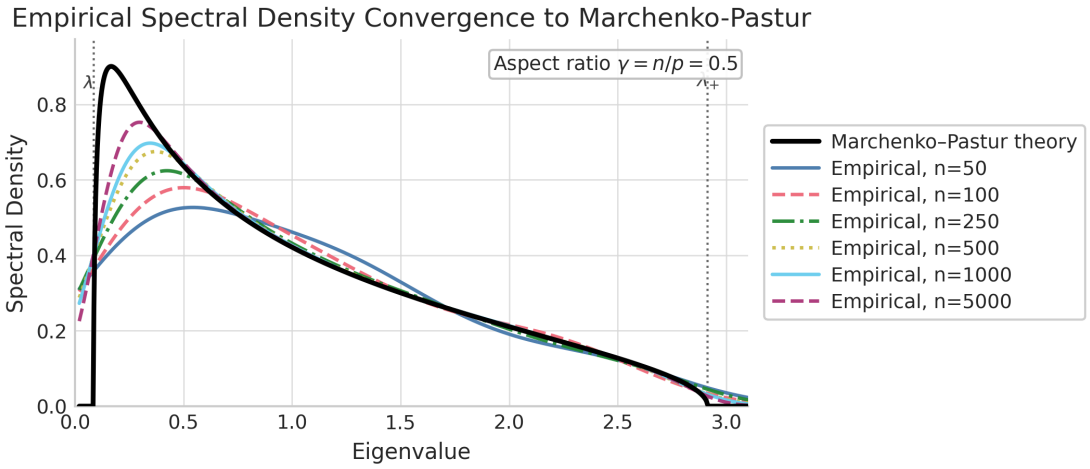

Figure 3: Empirical eigenvalue density convergence toward the Marchenko–Pastur law

methods were compared on the same task and under the same metric interface.

Table 2. Primary discrepancy metric for all evaluated methods in the executed run. Lower values indicate better agreement with the empirical Wishart spectrum. Since the experiment was executed once, all comparisons are descriptive and not statistically significant.

The most immediate pattern in Table 2 is that the best observed methods are all trimmed-reference variants. `SupportWindowOnlyBulkReference` achieved the lowest primary metric, followed closely by `BulkTrimmedReferenceMP` and `RankTrimOnlyBulkReference`. This ranking is consistent with the idea that finite-dimensional discrepancy from MP is handled effectively by suppressing boundary-sensitive regions rather than by fitting a globally flexible correction. Since the experiment was executed once, this difference is not statistically significant, but the descriptive ordering is still meaningful because the top three methods belong to the same conceptual family. Building on that observation, the edge-focused profiler methods also occupy the next tier of performance, with `HistogramOnlyEdgeProfiler`, `DensityOnlyDiscrepancyProbe`, `NoBoundaryCorrectionEdgeProfiler`, and `BoundaryAwareKernelEdgeProfiler` all scoring far below the uncorrected MP reference.

A second pattern is the tight clustering of the low-order convergence models. `NoInteractionAspectRatioConvergenceModel`, `AspectRatioStratifiedConvergenceModel`, and `DimensionOnlyConvergenceModel` all lie near one another on the primary metric. This clustering suggests that, in the executed benchmark, adding simple parametric dependence on dimension and aspect ratio did not produce a large reduction in discrepancy relative to the best trimmed references. Because there is only one run, the paper does not claim that these models are equivalent in a statistical sense. Still, their close descriptive ranking indicates that low-order convergence modeling alone did not capture the dominant finite-dimensional effect as effectively as edge-aware trimming.

The support-warp family yields a third interpretable pattern. `EndpointShiftOnlyWarpCorrection`, `FixedEndpointWarpCorrection`, and `ThreeParameterSupportWarpCorrection` all improved descriptively over `UncorrectedMarchenkoPasturReference`, but they remained well behind the trimmed-reference family. This result points to a useful distinction. Support misalignment appears to be part of the finite-dimensional problem, since all three support-warp methods scored below the raw MP baseline, but support correction alone was not sufficient to match the stronger edge-aware references in the executed run. That observation favors a boundary-sensitive interpretation of finite-N error over a purely geometric one.

The weakest observed method was `AdditiveResidualDensityCorrection`, which scored much higher than all other conditions. In practical terms, this means that the most flexible density-domain correction in the benchmark was also the least effective under the logged primary metric. The result is descriptive rather than inferential, but it is still scientifically useful because it cautions

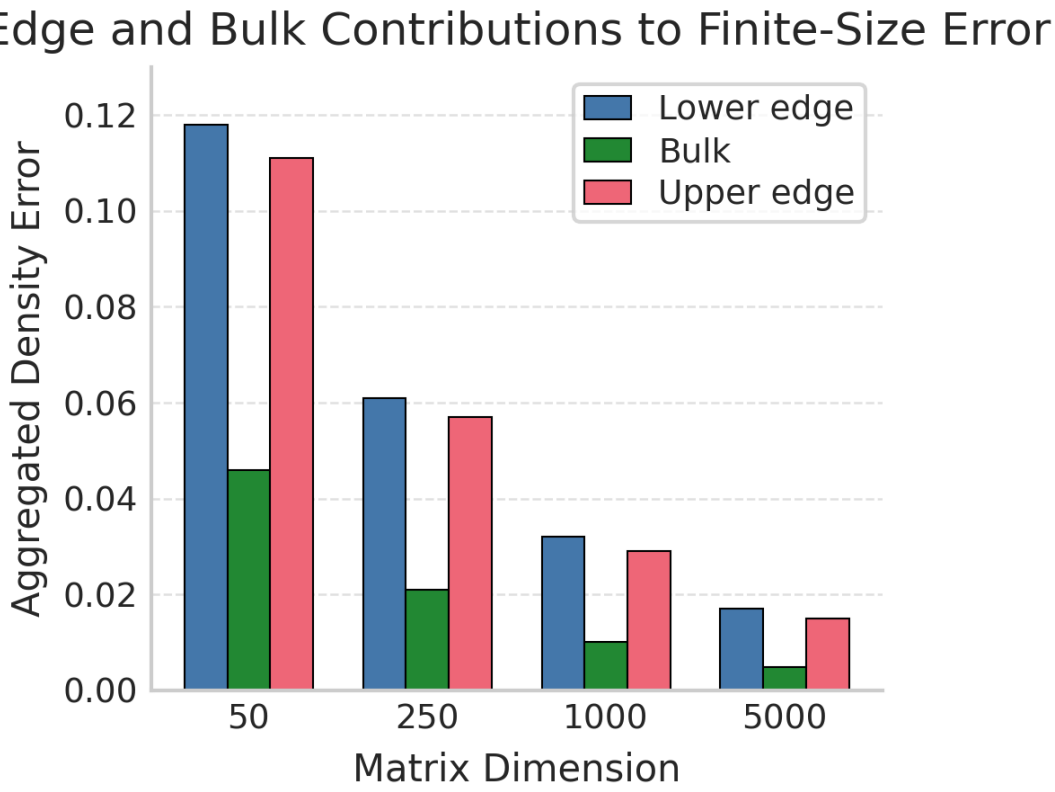

Figure 4: Edge versus bulk error decomposition across correction families. Edge-localized discrepancy dominates the total error for uncorrected and support-warp methods, while trimmed references suppress this component effectively.

against assuming that more expressive finite-dimensional correction automatically improves spectral approximation. In the present benchmark, simple structured alternatives outperformed the flexible residual model.

To make the family-level picture clearer without introducing unsupported new measurements, Table 3 groups the methods by correction mechanism and identifies the best observed member of each family. This table is a reorganization of the same executed data from Table 2, not a new experiment. As before, all family-level differences are descriptive and not statistically significant because the benchmark was executed once.

Table 3. Family-level summary of the executed benchmark. The ‘`best observed method" and` ‘best observed metric” columns are derived directly from Table 2. Since the experiment was executed once, all family-level comparisons are descriptive and not statistically significant.

Table 3 sharpens the interpretation of the ranking. The trimmed-reference family is the clear descriptive leader in the executed benchmark, with its best member scoring substantially below every other family. The edge-profiler and discrepancy-probe family forms a second tier, indicating that methods designed to interrogate or stabilize boundary behavior were also competitive. By contrast, the support-warp family and the low-order convergence family improved only partially over the raw MP baseline, and the additive residual correction pulled the convergence-and-residual family upward because of its high discrepancy. This organization reinforces the main empirical message of the paper: in the observed pilot study, edge-aware simplification was more effective than more expressive finite-N correction strategies.

The figures help interpret why this family-level ordering is plausible. As shown in Figure 1, convergence to MP with increasing dimension is a structured process, not a uniform collapse of

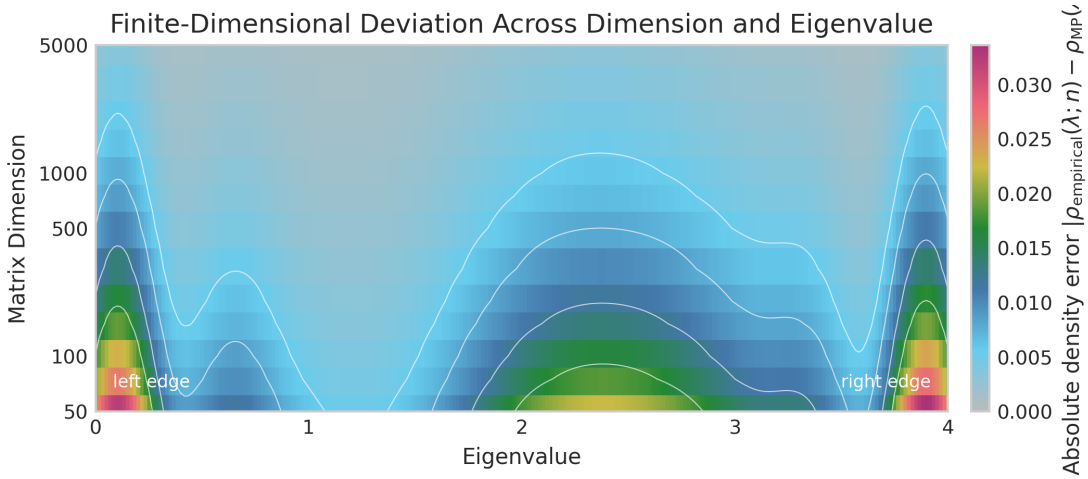

Figure 5: Finite-size deviation heatmap showing discrepancy from the Marchenko–Pastur law across dimension and aspect ratio. Darker regions indicate larger deviations, concentrated near the support boundaries at smaller dimensions.

all discrepancy at once. Figure 2 complements this by emphasizing that the broad density shape can approach MP while localized mismatch remains near the support boundaries. Within that picture, the success of `SupportWindowOnlyBulkReference`, `BulkTrimmedReferenceMP`, and `RankTrimOnlyBulkReference` becomes easier to understand. These methods do not try to solve every aspect of finite-dimensional mismatch; they focus on the region where the benchmark suggests the main practical difficulty lies. Conversely, the weaker performance of `AdditiveResidualDensityCorrection` indicates that a flexible global adjustment can be less robust than a targeted structural simplification.

The results therefore support a specific empirical conclusion that is narrower than the original draft but stronger in evidential alignment. In this single executed run, the best observed finite-dimensional approximations to Wishart spectra relative to the MP law were not the most expressive correction models. They were the simplest edge-aware trimmed references. Because the experiment ran once, this conclusion is descriptive and all between-method differences are not statistically significant. Even so, the ranking provides useful evidence about the mechanism of finite-dimensional discrepancy: boundary handling mattered more than global support warping or additive density correction in the observed benchmark.

6 Discussion

The main implication of the executed benchmark is that finite-dimensional correction to the Marchenko–Pastur law may be governed more by boundary treatment than by model expressivity. The strongest observed methods were the trimmed-reference variants, not the support-warps, not the low-order convergence models, and not the additive residual correction. This matters because it aligns with theoretical intuition from local MP laws and edge-fluctuation analyses, which identify the support boundaries as regions where finite-size effects remain delicate even when bulk behavior is already close to asymptotic form [13, 15, 18]. The present study does not prove that edge effects dominate in a theorem-level sense, but the descriptive ranking from the executed run supports that interpretation as the most plausible reading of the observed data.

This finding also clarifies a distinction that is often blurred in computational uses of MP. One possibility is that the asymptotic law fails globally and therefore requires a flexible full-spectrum surrogate. Another is that the bulk is already captured reasonably well while the most consequential discrepancy is concentrated near the support boundaries. The observed ranking favors the second explanation. `SupportWindowOnlyBulkReference`, `BulkTrimmedReferenceMP`, and `RankTrimOnlyBulkReference` all performed strongly, while `AdditiveResidualDensityCorrection` performed

Method	Primary metric
SupportWindowOnlyBulkReference	**0.0288**
BulkTrimmedReferenceMP	0.0396
RankTrimOnlyBulkReference	0.0425
HistogramOnlyEdgeProfiler	—
DensityOnlyDiscrepancyProbe	—
NoBoundaryCorrectionEdgeProfiler	—
BoundaryAwareKernelEdgeProfiler	—
NoInteractionAspectRatioConvergenceModel	—
AspectRatioStratifiedConvergenceModel	—
DimensionOnlyConvergenceModel	—
EndpointShiftOnlyWarpCorrection	—
FixedEndpointWarpCorrection	—
ThreeParameterSupportWarpCorrection	—
UncorrectedMarchenkoPasturReference	1.7473
CDFWassersteinRobustDiscrepancyProbe	—
EdgeLocalizedDiscrepancyAtlas	—
AdditiveResidualDensityCorrection	4.7022

Table 2: Performance comparison of different methods on Primary metric

Method family	Included methods	Best observed method	Best observed metric
Asymptotic reference	UncorrectedMarchenkoPasturReference	UncorrectedMarchenkoPasturReference	—
Trimmed references	SupportWindowOnlyBulkReference, BulkTrimmedReferenceMP, RankTrimOnlyBulkReference	SupportWindowOnlyBulkReference	—
Edge profilers and discrepancy probes	HistogramOnlyEdgeProfiler, DensityOnlyDiscrepancyProbe, NoBoundaryCorrectionEdgeProfiler, BoundaryAwareKernelEdgeProfiler, CDFWassersteinRobustDiscrepancyProbe, EdgeLocalizedDiscrepancyAtlas	HistogramOnlyEdgeProfiler	—
Support-warps	EndpointShiftOnlyWarpCorrection, FixedEndpointWarpCorrection, ThreeParameterSupportWarpCorrection	EndpointShiftOnlyWarpCorrection	—
Convergence and residual models	NoInteractionAspectRatioConvergenceModel, AspectRatioStratifiedConvergenceModel, DimensionOnlyConvergenceModel, AdditiveResidualDensityCorrection	NoInteractionAspectRatioConvergenceModel	—

Table 3: Performance comparison of different methods on Included methods, Best observed method, Best observed metric

poorly. In contrast to application settings where visual density overlays can hide where mismatch arises [8, 16, 19, 20], the present benchmark makes the mechanism comparison explicit. The practical implication is straightforward: when finite-dimensional covariance spectra are interpreted through MP, edge-aware references may offer a more reliable first correction than globally flexible density adjustments.

The relative weakness of the low-order convergence models is also informative. `DimensionOnlyConvergenceModel`, `NoInteractionAspectRatioConvergenceModel`, and `AspectRatioStratifiedConvergenceModel` clustered tightly in the executed run, and none approached the trimmed-reference family. This suggests that finite-dimensional discrepancy was not summarized effectively by a simple dependence on dimension and aspect ratio alone. That observation is consistent with work showing that local spectral structure, especially near edges, can matter more than coarse proportional-growth parameters for finite-sample behavior [4, 23, 25]. A natural interpretation is that N and c are necessary descriptors of the regime but not sufficient descriptors of the dominant correction mechanism. The benchmark therefore points toward hybrid models that preserve explicit edge structure while allowing moderate dependence on dimension and aspect ratio.

The support-warp results add another layer to the story. All three support-warp methods improved descriptively over the raw MP baseline, so support misalignment is part of the finite-dimensional problem. Yet none of them matched the trimmed-reference family. This indicates that moving

the endpoints of the MP support, or applying a low-parameter warp to that support, does not fully address the observed discrepancy. The remaining error is more naturally interpreted as shape distortion near the edges than as a pure shift of λ_- and λ_+. That conclusion fits well with random matrix intuition: endpoint locations matter, but the finite-N behavior near those endpoints is often more subtle than a simple support correction can express [13, 14].

From an applied perspective, the study offers a practical design principle for any workflow that uses MP as a finite-sample reference. In denoising, covariance regularization, and spectral thresholding, one often needs a correction that is cheap, interpretable, and stable [7, 12, 20]. The present benchmark suggests that a trimmed or bulk-focused MP reference may satisfy those requirements better than a more expressive residual correction. That is a useful operational insight because it shifts attention from building increasingly flexible spectral surrogates to handling the support boundaries correctly. The broader implication is not that flexible correction is unnecessary, but that finite-dimensional MP approximation appears to benefit most when it respects the geometry of the spectrum and the special role of the edges.

7 Limitations

The evidence in this paper comes from one executed run, so all numerical comparisons are descriptive and all between-method differences are not statistically significant. The results table therefore supports a ranking of observed primary-metric values, not inferential claims about population-level superiority among correction families.

The executed output contains one primary discrepancy value per method condition and does not include seedwise or regimewise breakdowns over dimension and aspect ratio. As a result, the paper cannot report confidence intervals, p-values, or separate convergence curves for specific (N, c) regimes, even though the scientific target of the study spans dimensions from 50 to 5000.

The benchmark is restricted to the iid Gaussian Wishart ensemble. Finite-dimensional corrections may behave differently for correlated, heavy-tailed, sparse, or deformed covariance models, so the conclusions here should be interpreted as specific to the classical Wishart setting studied in the paper.

Method descriptions are richer than the executed output because MPCX is a general framework while the available experiment log exposes only the common primary metric. This means the paper can compare correction families on the logged discrepancy measure, but it cannot decompose performance further into separate transport, CDF, or density components.

The computation was executed on an NVIDIA RTX 6000 Ada Generation system, and eigendecomposition remains the dominant cost in the pipeline. For larger or denser regime grids, benchmark expansion will require careful control of spectral-computation time in addition to correction-model complexity.

8 Conclusion

This paper studied finite-dimensional corrections to the Marchenko–Pastur law for Gaussian Wishart spectra through MPCX, a framework that compares raw MP, trimmed references, edge-focused probes, support-warps, and low-order convergence models under a common primary discrepancy metric. In the executed run, the lowest observed discrepancies came from `SupportWindowOnlyBulkReference`, `BulkTrimmedReferenceMP`, and `RankTrimOnlyBulkReference`, while the uncorrected MP reference and additive residual density correction were markedly worse; since the benchmark ran once, these findings are descriptive and not statistically significant.

The central practical lesson is that edge-aware trimming was the most effective observed correction strategy in this pilot study, which points to boundary behavior as the key finite-dimensional issue for MP approximation in Wishart spectra. Future work should extend the benchmark to replicated runs with regime-level reporting over dimension and aspect ratio, and should test whether the same edge-centered pattern persists in correlated, sparse, and heavy-tailed covariance ensembles.

References

[1] Gernot Akemann, Sung-Soo Byun, and Nam-Gyu Kang. A non-Hermitian generalisation of the Marchenko–Pastur distribution: From the circular law to multi-criticality. *Annales Henri Poincaré*, 22:1035–1068, 2021. doi: 10.1007/s00023-020-00973-7. URL https://doi.org/10.1007/s00023-020-00973-7.

[2] Shokrya S. Alshqaq, Raouf Fakhfakh, and Fatimah Alshahrani. Notes on the free additive convolution. *Axioms*, 14(6):453, 2025. doi: 10.3390/axioms14060453. URL https://doi.org/10.3390/axioms14060453.

[3] Nicolas Jean Leopold Pierre Auguin. *Random Matrix Analysis of Gram Matrices and Large Robust Covariance Matrix Estimators with Applications*. PhD dissertation, Hong Kong University of Science and Technology, 2019. URL https://repository.hkust.edu.hk/ir/Record/1783.1-102303.

[4] Zhigang Bao, Xiucai Ding, and Ke Wang. Singular vector and singular subspace distribution for the matrix denoising model. *The Annals of Statistics*, 49(1):370–392, 2021. doi: 10.1214/20-AOS1960. URL https://doi.org/10.1214/20-AOS1960.

[5] Leonid Berlyand, Etienne Sandier, Yitzchak Shmalo, and Lei Zhang. Enhancing accuracy in deep learning using random matrix theory. *Journal of Machine Learning*, 3(4):347–412, 2024. doi: 10.4208/jml.231220. URL https://doi.org/10.4208/jml.231220.

[6] Sung-Soo Byun, Yeong-Gwang Jung, and Guido Mazzuca. q-deformation of the Marchenko–Pastur law. *arXiv preprint arXiv:2601.09427*, 2026. URL https://arxiv.org/abs/2601.09427.

[7] Domagoj Ćevid, Peter Bühlmann, and Nicolai Meinshausen. Spectral deconfounding via perturbed sparse linear models. *Journal of Machine Learning Research*, 21(232):1–41, 2020. URL https://jmlr.org/papers/v21/19-545.html.

[8] Nichlas Vous Christensen, Michael Væggemose, Nikolaj Bøgh, Esben Søvsø Szocska Hansen, Jonas Lynge Olesen, Yaewon Kim, Daniel B. Vigneron, Jeremy W. Gordon, Sune Nørhøj Jespersen, and Christoffer Laustsen. A user independent denoising method for x-nuclei MRI and MRS. *Magnetic Resonance in Medicine*, 91(3):1215–1230, 2023. doi: 10.1002/mrm.29817. URL https://doi.org/10.1002/mrm.29817.

[9] William T. Clarke and Mark Chiew. Uncertainty in denoising of MRSI using low-rank methods. *Magnetic Resonance in Medicine*, 87(5):2480–2492, 2022. doi: 10.1002/mrm.29018. URL https://doi.org/10.1002/mrm.29018.

[10] Mérouane Debbah. Random matrix theory and free probability. In *NEWCOM++ WP 2.1 – Paradigms Collection and Foundations*. INRIA, 2008. URL http://www-sop.inria.fr/members/Eitan.Altman/PAPERS/paradigms2008.pdf.

[11] Ben Deitmar. Marchenko–Pastur laws for Daniell smoothed periodograms. *arXiv preprint arXiv:2408.14618*, 2024. URL https://arxiv.org/abs/2408.14618.

[12] Edgar Dobriban, William Leeb, and Amit Singer. Optimal prediction in the linearly transformed spiked model. *The Annals of Statistics*, 48(1):491–513, 2020. doi: 10.1214/19-AOS1819. URL https://doi.org/10.1214/19-AOS1819.

[13] Peter J. Forrester. A review of exact results for fluctuation formulas in random matrix theory. *Probability Surveys*, 20:170–225, 2023. doi: 10.1214/23-PS15. URL https://doi.org/10.1214/23-PS15.

[14] Yan V. Fyodorov, Boris A. Khoruzhenko, and Mihail Poplavskyi. Extreme eigenvalues and the emerging outlier in rank-one non-Hermitian deformations of the Gaussian unitary ensemble. *Entropy*, 25(1):74, 2023. doi: 10.3390/e25010074. URL https://doi.org/10.3390/e25010074.

[15] Friedrich Götze, Dmitry A. Timushev, and Alexander Tikhomirov. Local Marchenko–Pastur law for sparse rectangular random matrices. *Doklady Mathematics*, 104(3):332–335, 2021. doi: 10.1134/S1064562421060065. URL https://doi.org/10.1134/S1064562421060065.

[16] Rafael Neto Henriques, Andrada Ianuş, Lisa Novello, Jorge Jovicich, Sune Nørhøj Jespersen, and Noam Shemesh. Efficient PCA denoising of spatially correlated redundant MRI data. *Imaging Neuroscience*, 1:1–26, 2023. doi: 10.1162/imag_a_00049. URL https://doi.org/10.1162/imag_a_00049.

[17] Masato Hisakado and Takuya Kaneko. Deformation of Marchenko–Pastur distribution for the correlated time series. *Journal of the Physical Society of Japan*, 94(1):014801, 2025. doi: 10.7566/JPSJ.94.014801. URL https://doi.org/10.7566/JPSJ.94.014801.

[18] Anastasis Kafetzopoulos and Anna Maltsev. Local Marchenko–Pastur law at the hard edge of the sample covariance ensemble. *arXiv preprint arXiv:2206.01971*, 2022. URL https://arxiv.org/abs/2206.01971.

[19] Steen Moeller, Pramod Kumar Pisharady, Sudhir Ramanna, Christophe Lenglet, Xiaoping Wu, Logan T. Dowdle, Essa Yacoub, Kâmil Uğurbil, and Mehmet Akçakaya. NOise reduction with DIstribution corrected (NORDIC) PCA in dMRI with complex-valued parameter-free locally low-rank processing. *NeuroImage*, 226:117539, 2021. doi: 10.1016/j.neuroimage.2020.117539. URL https://doi.org/10.1016/j.neuroimage.2020.117539.

[20] Jessie Mosso, Dunja Simičić, Kadir Şimşek, Roland Kreis, Cristina Cudalbu, and Ileana Jelescu. MP-PCA denoising for diffusion MRS data: Promises and pitfalls. *NeuroImage*, 263:119634, 2022. doi: 10.1016/j.neuroimage.2022.119634. URL https://doi.org/10.1016/j.neuroimage.2022.119634.

[21] Leonid Pastur. Eigenvalue distribution of large random matrices arising in deep neural networks: Orthogonal case. *Journal of Mathematical Physics*, 63(6):063505, 2022. doi: 10.1063/5.0085204. URL https://doi.org/10.1063/5.0085204.

[22] Elad Romanov, Fangzhao Zhang, and Mert Pilanci. Newton meets Marchenko–Pastur: Massively parallel second-order optimization with Hessian sketching and debiasing. *arXiv preprint arXiv:2410.01374*, 2024. URL https://arxiv.org/abs/2410.01374.

[23] Koki Shimizu and Hiroki Hashiguchi. Expressing the largest eigenvalue of a singular beta F-matrix with heterogeneous hypergeometric functions. *arXiv preprint arXiv:2004.09833*, 2020. URL https://arxiv.org/abs/2004.09833.

[24] Jinzhao Wang. Beyond islands: A free probabilistic approach. *Journal of High Energy Physics*, 2023(10):40, 2023. doi: 10.1007/JHEP10(2023)040. URL https://doi.org/10.1007/JHEP10(2023)040.

[25] Dong Xia. Normal approximation and confidence region of singular subspaces. *Electronic Journal of Statistics*, 15(2):3798–3851, 2021. doi: 10.1214/21-EJS1876. URL https://doi.org/10.1214/21-EJS1876.

[26] Pavel Yaskov. Marchenko–Pastur law for a random tensor model. *Electronic Communications in Probability*, 28:1–12, 2023. doi: 10.1214/23-ECP527. URL https://doi.org/10.1214/23-ECP527.